Sensors and Actuators Reports 4 (2022) 100101

Contents lists available at ScienceDirect

Sensors and Actuators Reports

journal homepage: www.sciencedirect.com/journal/sensors-and-actuators-reports

A rapid and sensitive fluorescence biosensor for Hg^{2+} detection in environmental samples

Yunpeng Xing [a,b,1], Boyuan Xue [b,1], Peishi Qi [a,*], George Y. Chen [c], Xiaohong Zhou [b,*]

[a] State Key Laboratory of Urban Water Resource and Environment, School of Environment, Harbin Institute of Technology, Harbin 150090, China
[b] State Key Joint Laboratory of ESPC, School of Environment, Tsinghua University, Beijing 100084, China
[c] Shenzhen Key Laboratory of Photonic Devices and Sensing Systems for Internet of Things, Guangdong and Hong Kong Joint Research Centre for Optical Fibre Sensors, Shenzhen University, Shenzhen 518060, China

ARTICLE INFO

Keywords:
T-Hg^{2+}-T mismatch
SYBR Green I
Mercury-specific oligonucleotide
Mercury detection
Fluorescence intensity

ABSTRACT

As a significant environmental pollutant, Hg^{2+} has gained widespread concern around the world. In our work, a rapid and elegant fluorescence method based on SYBR GREEN I (SGI) and mercury-specific oligonucleotide (MSO) has been developed for detection of Hg^{2+}. Utilizing the T-Hg^{2+}-T mismatch principle, MSO forms a double-stranded hairpin structure, which can readily embed SGI and produce strong fluorescence. Under optimized conditions including MSO concentration, dye/MSO base ratio, pH value, ionic strength, reaction time and incubation time, a wide linear range (10–100 nM) and a low limit of detection (0.68 nM) were demonstrated. Almost no statistically significant interference for Hg^{2+} detection was observed among the possible coexisting substances in the water samples, including 15 factors. The recoveries of the three environmental water samples were in the range of 82.8% to 101.8%, indicating that the method was only weakly affected by the environmental matrix and could be applied to the detection of Hg^{2+} in environmental water samples. This method features potentially low cost, rapid processing, and convenient operation, which indicates considerable promise in practical Hg^{2+} monitoring.

1. Introduction

With the rapid development of industrialization and expansion of urbanization, the extent of global water pollution is becoming increasingly severe. Generally, heavy metal pollution is characterized by high toxicity, easy accumulation, difficult degradation and difficult treatment. Although at low concentrations, heavy metals can still pose a serious threat to human health, including stunted growth, cancer, organ disease, nervous system disorders and even death [1]. Among them, cadmium, mercury, lead, and arsenic are the most common and toxic heavy metal pollutants [2]. Atomic Absorption Spectrophotometer (AAS), Inductively Coupled Plasma-Atomic Emission Spectrometer (ICP-AES), and Inductively Coupled Plasma Mass Spectrometry (ICP-MS) are the standard methods for the quantification of trace heavy metal ions in water environments and food industries. These methods possess the advantages of high precision and low limit of detection, but the complex pretreatments, time-consuming processes, high detection cost, and requirement of professional operators limit their versatile applications in practice [3]. In addition, these methods greatly rely on large-sized laboratory equipment, which makes it difficult to realize real-time and in-field measurements [4]. Recently, it is reported that electrochemical anodic stripping voltammetry can be used to determine the concentration of heavy metals, exhibiting high sensitivity and low detection cost. However, in addition to the need of professional operators, the employment of heavy metals as electrodes will introduce additional pollution to the natural environment [5, 6]. Therefore, many initiatives have been undertaken to rapidly detect heavy metals in field by colorimetric, optical and electrochemical sensors [7–13].

Mercury, is a highly toxic metal with global emissions of around 19,000 tons per year. Long-term exposure to mercury can cause adverse effects on the brain, kidney, immune system, and other physiological organs. The vast majority of mercury emissions come from the manufacturing and processing activities of human beings, such as the burning of coal. The most common toxic mercury state in natural water sources is water-soluble divalent mercury ion (Hg^{2+}) [14]. Therefore, the development of simple, rapid, highly sensitive, and highly specific

* Corresponding authors.
E-mail addresses: qipeishi@163.com (P. Qi), xhzhou@mail.tsinghua.edu.cn (X. Zhou).
[1] The authors equally contributed to this work

https://doi.org/10.1016/j.snr.2022.100101
Received 9 February 2022; Received in revised form 2 April 2022; Accepted 5 April 2022
Available online 13 April 2022

Table 1
Common interference factors with the concentrations under the majority of the most unfavorable conditions existed in environmental water

Interference factors			Concentrations
Metal ions	1	Pb^{2+}	0.1 mg/L Pb^{2+} in $Pb(NO_3)_2$
	2	Cu^{2+}	1.0 mg/L Cu^{2+} in $Cu(NO_3)_2$
	3	Ni^{2+}	0.1 mg/L Ni^{2+} in $Ni(NO_3)_2$
	4	Zn^{2+}	2.0 mg/L Zn^{2+} in $Zn(NO_3)_2$
	5	Al^{3+}	0.2 mg/L Al^{3+} in $Al(NO_3)_3$
	6	Mn^{2+}	0.2 mg/L Mn^{2+} in $Mn(NO_3)_2$
	7	Ag^{+}	0.05mg/L Ag^{+} in $AgNO_3$
	8	MIX	All of above
Anions	9	NO_3^-	10 mg/L NO_3^- in $NaNO_3$
	10	SO_4^{2-}	250 mg/L SO_4^{2-} in Na_2SO_4
	11	Cl^-	300 mg/L Cl^- in NaCl
	12	F^-	10 mg/L F^- in NaF
Hardness	13	Ca^{2+}	400 mg/L Ca^{2+} in $Ca(NO_3)_2$
	14	Mg^{2+}	240 mg/L Mg^{2+} in $Mg(NO_3)_2$
Other	15	ClO^-	4.0 mg/L NaClO

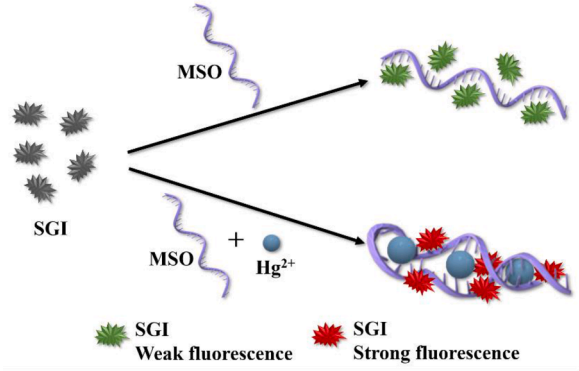

Fig 1. Sensing schematic diagram of the turn-on fluorescence detection of Hg^{2+}.

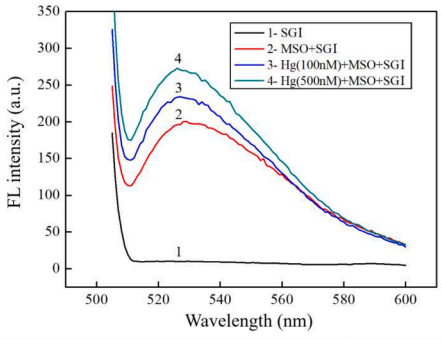

Fig 2. Fluorescence spectra of solution of MSO and SGI at different concentration of Hg^{2+}. Curve 1: 1 × SGI; curve 2: 1 μM MSO + 1 × SGI; curve 3: 1 μM MSO + 1 × SGI + 100 nM Hg^{2+}; curve 4: 1 μM MSO + 1 × SGI + 500 nM Hg^{2+}.

detection technologies for Hg^{2+} has important theoretical and practical value. A large number of studies have shown that at the molecular level, some heavy metal ions can interact with specific gene sequences to change their spatial structure [15]. The relationship between structure and performance provides a convenient way for rapid and specific identification of heavy metal ions. A class of nucleic acid molecules with specific biological functions, such as aptamer, DNAzyme, Aptazyme (complex of aptamer and DNAzyme), etc., screened *in vitro* by the Systematic Evolution of Ligands by Exponential Enrichment (SELEX) technique, were discovered and synthesized [16], and applied to the detection of heavy metal ions [17–20]. In 2004, Ono and Togashi discovered that Hg^{2+} could bind between two thymine (T) bases, causing T-Hg^{2+}-T mismatch, and subsequently designed a fluorescent Hg^{2+} sensor based on this theory [17]. In this design, the T-rich DNA, labeled at both ends, was folded into a hairpin structure in the presence of Hg^{2+}, resulting in the reduction of fluorescence intensity. Since then, Hg^{2+} biosensing technologies based on T-rich functional nucleic acids have gradually become a hot topic in environmental and analytical sciences. Compared with antibodies, the traditional affinity recognition material, functional nucleic acids can be synthesized artificially and screened *in vitro* without considering whether the target has immunogenicity, containing the advantages of low production cost and stable performance [21,22].

In order to further enhance the sensitivity of T-Hg^{2+}-T mismatch sensing detection, methods based on photoinduced electron transfer [23], graphene oxide (GO) [24], molecular beacons [25], and DNA embedded dyes [26] have been demonstrated to show low background signals compared with other methods. SYBR Green I (SGI), whose sensitivity is 25–100 times higher than that of ethidium bromide, is an asymmetric cyanine dye used as a nucleic acid stain in molecular biology. SGI is a fluorescent dye that can be embedded into double-stranded DNA (dsDNA) and form high binding affinity. Under excitation light of 497 nm, the fluorescence intensity of SGI binding with dsDNA is a factor of 11 or higher than that of single-stranded DNA (ssDNA), which is weakly affected by acidity, volume, and time, making it possible for relating the fluorescence intensity of SGI to the amount of dsDNA. SGI has been successfully used in DNA qualitative and quantitative techniques, such as gel electrophoresis and PCR technology [27].

In this work, we exploit the characteristic that Hg^{2+} can specifically bind thymine on a DNA sequence to form a T-Hg^{2+}-T double chain, select T-rich ssDNA sequence as the recognition element, and use embedded dye SGI as the indicator. According to the changes of SGI fluorescence signal in response to the structural change of the mercury-specific oligonucleotide (MSO) before and after the addition of Hg^{2+}, our rapid and practical fluorescence biosensor can pave the way for achieving high-sensitivity detection of Hg^{2+} in water. Although previous work reported the label-free fluorescence assay for one-step detection of Hg^{2+} via the T-rich ssDNA sequence and dye SGI [28], we systematically investigate the effects of the major aqueous matrix on the biosensor performance, including 15 common interference factors in the aqueous system and the corresponding tolerance level of this method. The significant improvement of understanding the practicality of the rapid and elegant fluorescence method for Hg^{2+} detection in environmental samples will greatly promote and provide strong data for its down-stream applications of this method.

2. Materials and methods

2.1. Materials and apparatus

Mercury-specific oligonucleotide (MSO): DNA sequence (5'-TTC TTT CTT CCCC TTG TTT GTT-3'), Shanghai Sangon Biotechnology Co., Ltd. (Shanghai, China).

Compared chain (T_{33}): DNA sequence (5'-TTT TTT TTT TTT TTT TTT TTT TTT TTT TTT TTT TTT-3'), Shanghai Sangon Biotechnology Co., Ltd. (Shanghai, China).

SYBR Green I (SGI): 10000 ×, Beijing Solarbio Science & Technology Co., Ltd. (Beijing, China).

3-(N-Morpholino) propanesulfonic acid (MOPS): Mediatech Co., Ltd. (Shanghai, China).

Interfering substance: $Pb(NO_3)_2$, $Cu(NO_3)_2$, $Ni(NO_3)_2$, $Zn(NO_3)_2$, $Al(NO_3)_3 \bullet 9H_2O$, $Mn(NO_3)_2$, $AgNO_3$, $NaNO_3$, Na_2SO_4, NaCl, NaF, $Ca(NO_3)_2$, $Mg(NO_3)_2$, NaClO, AR, Sinopharm Chemical Reagent Co., Ltd (Beijing, China).

Hg^{2+} standard solution: $Pb(NO_3)_2$, AR, Sinopharm Chemical Reagent Co., Ltd (Beijing, China).

Fluorescent emission spectra: F-7000 fluorescence spectrometer (Hitachi, Tokyo, Japan).

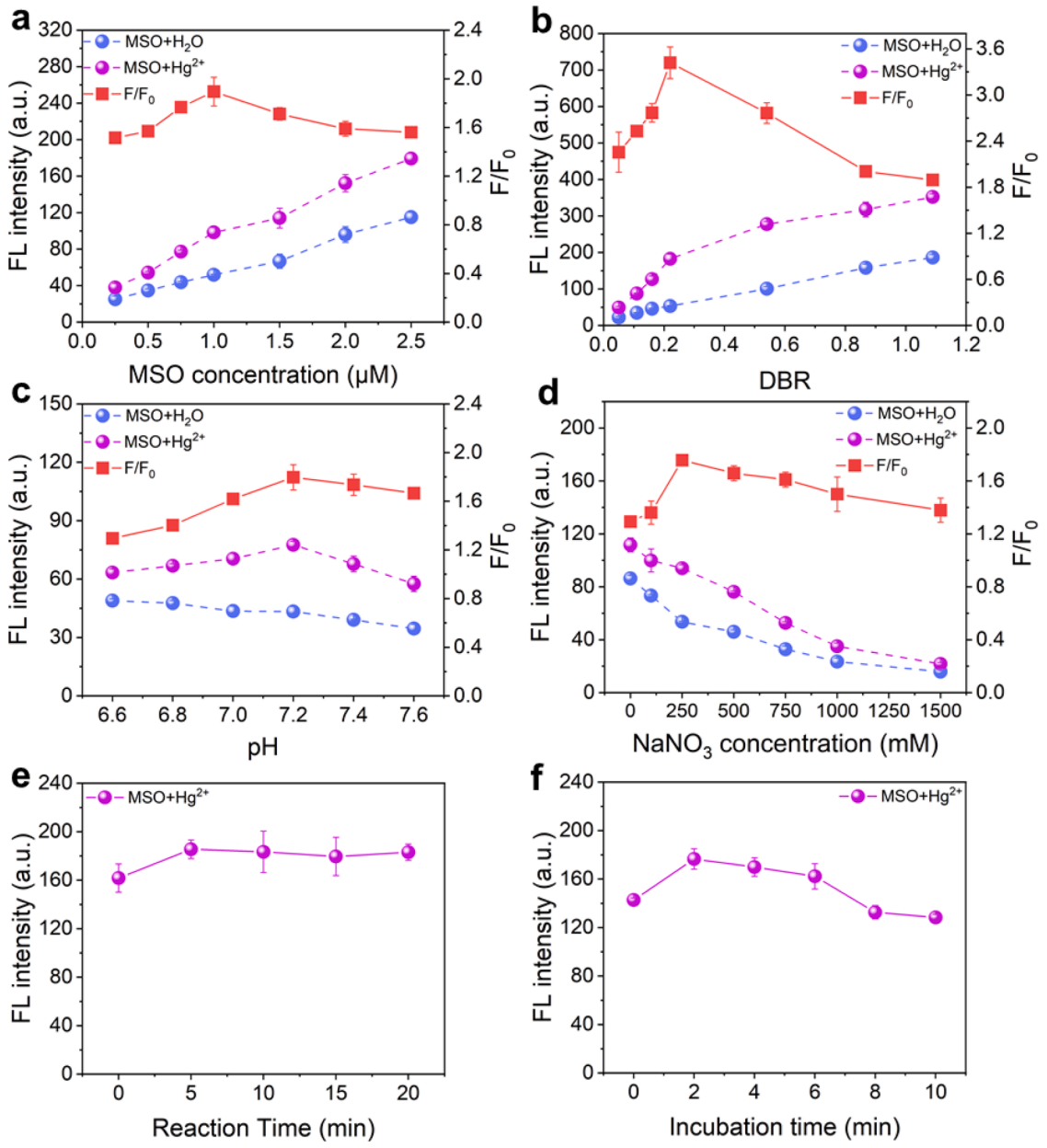

Fig 3. Effect of (a) MSO concentration; (b) dye/MSO base ratio (DBR); (c) pH value; (d) ionic strength; (e) reaction time; (f) incubation time on fluorescence intensity for Hg^{2+} detection.

2.2. Solution preparation

Hg^{2+} solution: Hg^{2+} standard solution was step by step diluted to 5 μM with ultrapure water, and kept at 4°C for storage.

MOPS buffer solution: 2.0926 g MOPS powder was dissolved in 100 mL ultrapure water and mixed evenly. The prepared concentration was 500 mM, and the solution was kept at 4°C for storage. A certain amount of $NaNO_3$ was added into MOPS buffer to keep ion strength.

SGI solution: 10000 × SGI solution was diluted to 100 × SGI with dimethyl sulfoxide (DMSO) step by step as the reserve solution, which was kept away from light at -20°C for storage. When using, the reserve solution was step by step diluted to 1 × SGI solution with ultrapure water.

MSO pre-treatment: MSO was very light and attached to the tube wall in a dry film form. So before preparing the solution, it was centrifuged at 12000 rpm for 2 min. Then it was added to ultrapure water to form a 100 μM solution, mixed evenly and restored at -20°C as the reserve solution.

2.3. Feasibility for Hg2+ detection using MSO and SGI

10 μL MSO (1 μM), 10 μL MOPS buffer (100 mM) and 80 μL appropriate concentration of Hg^{2+} (0, 1, 5, 7.5, 10, 20, 30, 40, 50, 75, 100, 120, and 150 nM) were mixed and reacted at room temperature for 10 min to form the T-Hg^{2+}-T complex. Then 5 μL 1 × SGI was added into the mixture and incubated at room temperature for 2 min before the fluorescence was measured. Finally, ultrapure water was added to keep the mixture volume of 800 μL. After adding, fluorescence was detected by a fluorescence spectrophotometer. Fluorescence (FL) intensity was recorded at 520 nm with an excitation wavelength of 494 nm.

2.4. Optimization for Hg2+ detection conditions using MSO and SGI

In initial experiments, the reaction conditions were set as follows:

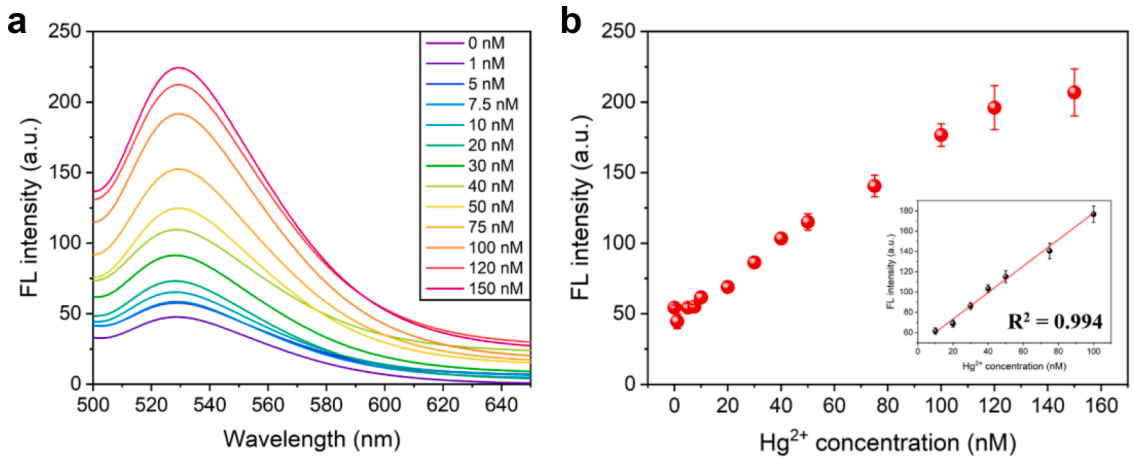

Fig 4. Calibration curve for detection of Hg^{2+} from 0–150 nM. (a) Typical fluorescent spectra and (b) the corresponding FL intensities (The inset shows a linear relationship between FL and Hg^{2+} concentration) under different Hg^{2+} concentration.

Table 2
Performance comparison of the developed biosensor with other reported technologies

Method	Sensing mode	Quantification range	LOD	Refs.
Sybr Green I and T-Hg^{2+}-T	Fluorescent	5-1000 nM	3 nM	[28]
Sybr Green I and T-Hg^{2+}-T	Fluorescent	0-66.4 nM	1.33 nM	[30]
Fluorescein, AuNPs and T-Hg^{2+}-T	Fluorescent	20-1000 nM	16.0 nM	[31]
Fluorescein, carbon nanotubes and T-Hg^{2+}-T	Fluorescent	50-8000 nM	14.5 nM	[32]
AgNPs-tryptophan nanoconjugate and Hg^{2+}	Colorimetric	20-100 nM	6.64 nM	[37]
Fe@Ag-starch nanoparticle	Surface plasmon resonance	1-1000 nM	1.48 nM	[38]
Copper nanoclusters and Hg-S bond	Fluorescent	1-500 nM	0.3 nM	[39]
Copper nanoparticles and Hg-S bond	Fluorescent	0.5-100 nM	0.1 nM	[40]
AuNPs functionalized with RhG and Hg-S bond	Fluorescent	2-12 nM	2 nM	[41]
This work	Fluorescent	10-100 nM	0.68 nM	

C_{Hg} = 40 nM, C_{MSO} = 1 μM, SGI = 1 ×, 100 mM MOPS buffer (including 250 mM $NaNO_3$), pH = 7.2, T-Hg^{2+}-T reaction time of 5 min, and SGI and MSO-Hg^{2+} incubation time of 2 min. In subsequent experiments, the parameters were changed to find the optimal reaction conditions. Optimized conditions including: MSO concentration, dye/MSO base ratio, pH value, ionic strength, reaction time and incubation time. Fluorescence intensity with and without Hg^{2+} and its ratio F/F_0 were used as dependent variable for detection. In order to minimum the sensitivity, reaction conditions stated above were optimized to maximum the F/F_0 ratio. Notably, considering that adjusting the temperature of the environmental samples higher or lower room temperature is not so easy, we suggested to keep the samples to room temperature before detection.

2.5. *Selectivity of Hg^{2+} detection using MSO and SGI*

The selectivity of the present system for Hg^{2+} detection was evaluated by investigating the effects of common interference factors in the aqueous matrix. The interference factors include 15 items (**Table 1**) with the concentrations under the majority of the most unfavorable conditions. To verify the selectivity of this method, response tests and coexistence interference tests were carried out, i.e., fluorescence intensity was recorded both in the presence and absence of Hg^{2+}.

2.6. *Recovery of Hg^{2+} detection using MSO and SGI*

To test the performance of this method in a real measurement environment and the matrix effect in the natural water environment, this study selected three kinds of environmental water to carry out a spiked recovery experiment, including two types of surface water (Danjiangkou Reservoir and Hetang Lake at Tsinghua University), and groundwater with a hardness of 290–350mg/L calcium carbonate sampled from hundreds of meters below Tsinghua University grounds. Danjiangkou Reservoir is the water source of the middle route of the South-to-North Water Diversion Project. Hetang Lake is a small lake at Tsinghua University.

A few pre-treatments were applied before the measurement, including boiling the water samples to precipitate the carbonate hardness, cooling the samples to room temperature and filtering them through a filter with a 0.22 μm nylon membrane, and then diluting twice using ultra-pure water before the recovery experiments [29]. Within the linear range of detection, the spiked concentrations were 10, 50 and 100 mg/L, respectively. Each sample was tested in parallel twice before and after spiking, and the recoveries were calculated, respectively. Besides, the spiked samples were analyzed by using the inductively coupled plasma mass spectrometry (ICP-MS) for comparison.

3. Results and Discussion

3.1. *Detection mechanism*

In this study, T-rich DNA (MSO) was used as the recognition element and SGI as the fluorescence indicator. The SGI was reported to efficiently discriminate MSO and MSO/Hg^{2+} complex on the principle of mercury-driven T-T DNA mismatch, which was firstly reported in 2004 [17,30], therefore an unlabeled fluorescent aptamer sensor was designed for Hg^{2+} detection (**Fig 1**). Notably, the MSO sequence has been adopted by many researchers for Hg^{2+} specific recognition [17,30 32]. When there is no presence of Hg^{2+} in the system, SGI can only bind to the single chain aptamer through electrostatic interaction, which emits very weak fluorescence. After the addition of Hg^{2+}, DNA can be folded into a stable intramolecular T-Hg^{2+}-T double-stranded structure, due to the fact that Hg^{2+} can selectively bind to two thymine (T) bases. SGI can interact with T-Hg^{2+}-T double chain and emit strong fluorescence through

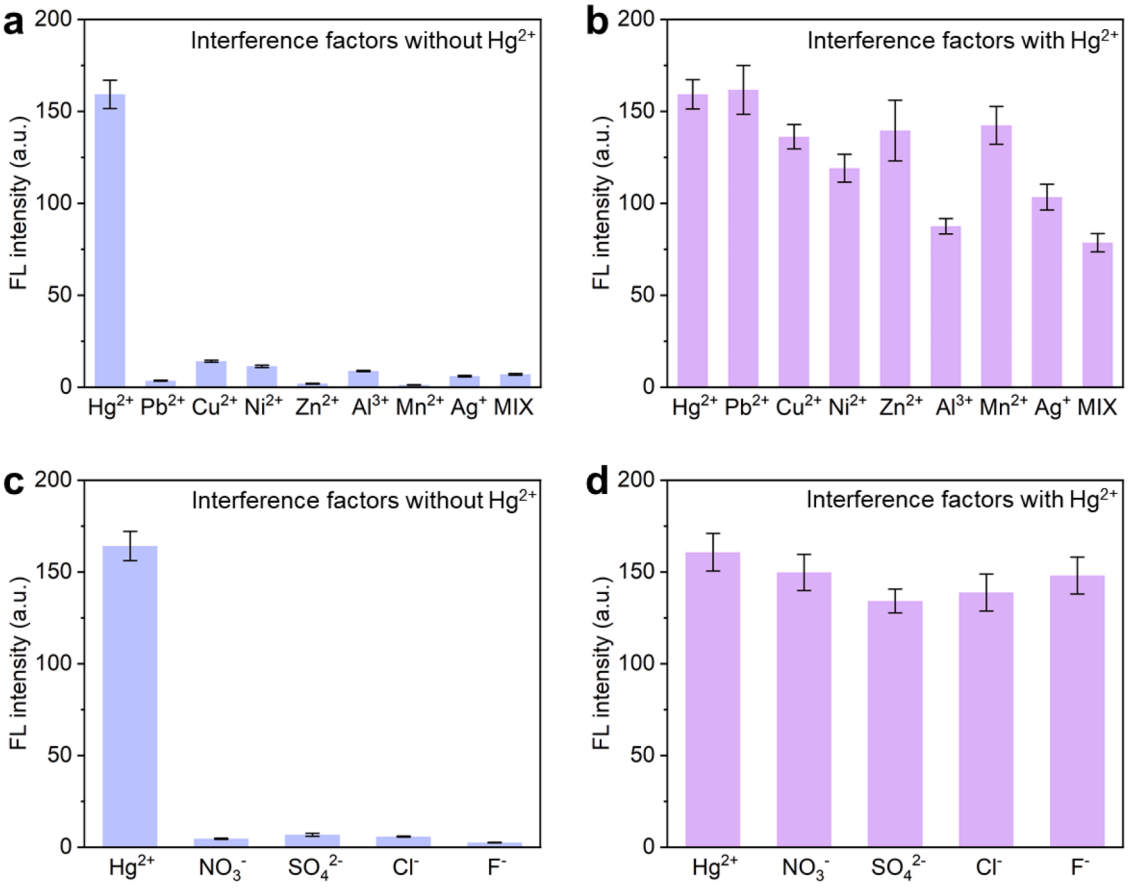

Fig 5. Selectivity of the proposed bioassay against different interference ions. (a) metal ions without Hg^{2+}; (b) metal ions with Hg^{2+}; (c) anions without Hg^{2+}; and (d) anions with Hg^{2+}.

embedding and small groove bonding. Therefore, when MSO changes from single chain to double chain configuration similar to hairpin structure, SGI fluorescence can be enhanced, and its increased intensity is related to the concentration of Hg^{2+}, thus realizing the quantitative detection of Hg^{2+}.

3.2. Feasibility of the method for Hg^{2+} detection

Fig 2 shows the fluorescence change of SGI in the absence and presence of different conditions of Hg^{2+}. In the absence of Hg^{2+}, the solution of SGI only showed a very weak fluorescence (curve 1). Upon the addition of MSO, the fluorescence of mixture increased slightly (curve 2), illustrating that the randomly coiled MSO interacted weakly with SGI. However, in the presence of 100 nM and 500 nM Hg^{2+} respectively, the fluorescence of SGI/MSO complex increased continually (curve 3, 4), also with the increase of the concentration of Hg^{2+}, the fluorescence of mixture increased consequently. The discrimination between SGI-MSO and SGI-Hg^{2+}-MSO indicated that the MSO also had folded into a hairpin-like structure and interacted strongly with SGI, which made the method possible to achieve the detection of Hg^{2+}.

3.3. Optimization of experimental conditions

3.3.1. Optimization of MSO concentration and dye/MSO base ratio

The concentration of MSO had a large influence on the function of the sensing system SGI/MSO/Hg^{2+} [11]. The appropriate MSO concentration could maximize the function of the sensing system. Firstly, the concentration of MSO was optimized (Fig 3a), and other reaction conditions were set as follows: C_{Hg} = 40 nM, SGI = 1 ×, 100 mM MOPS buffer (including 250 mM $NaNO_3$), pH = 7.2, T-Hg^{2+}-T reaction time of 5 min, and SGI and MSO-Hg^{2+} incubation time of 2 min. With the increase of MSO concentration, the fluorescence intensity with and without Hg^{2+} both increased, but with Hg^{2+}, the slope of fluorescence increase was steeper (higher gradient). Besides, with the increase of MSO concentration, the corresponding F/F_0 ratio firstly increased. When MSO concentration exceeded 1μM, the ratio began to decrease. Therefore, 1μM MSO concentration was selected as the optimal concentration.

SGI determines the fluorescent intensity of this system and hence its concentration affects the sensitivity of the system [11]. Since MSO concentration was set as 1μM, dye/base ratio (DBR) optimization was performed by changing SGI concentration (Fig 3b). Other reaction conditions were set as follows: C_{Hg} = 40 nM, 100 mM MOPS buffer (including 250 mM $NaNO_3$), pH = 7.2, T-Hg^{2+}-T reaction time of 5 min, and SGI and MSO-Hg^{2+} incubation time of 2 min. With the increase of DBR value, fluorescence intensity increased both in the groups with and without the addition of Hg^{2+}, and the slope of fluorescence increase was larger with the addition of Hg^{2+}, and the corresponding F/F_0 ratio reached the maximum when DBR value was 0.22. Considering the sensitivity and signal noise ratio (SNR) of the system, SGI 1 × was finally selected, i.e., DBR 0.22 is the best experimental parameter.

3.3.2. Optimization of pH value and ionic strength

A suitable pH is essential for a fluorescence molecule due to protonation and deprotonation [33]. The effect of pH on Hg^{2+} detection was analyzed (Fig 3c). The reaction conditions were set as follows: C_{Hg} = 40 nM, SGI = 1 ×, 100 mM MOPS buffer (including 250 mM $NaNO_3$), T-Hg^{2+}-T reaction time of 5 min, and SGI and MSO-Hg^{2+} incubation time of 2 min. When pH increased from 6.6 to 7.6, the fluorescence of MSO-H_2O system decreased slightly, while the fluorescence of

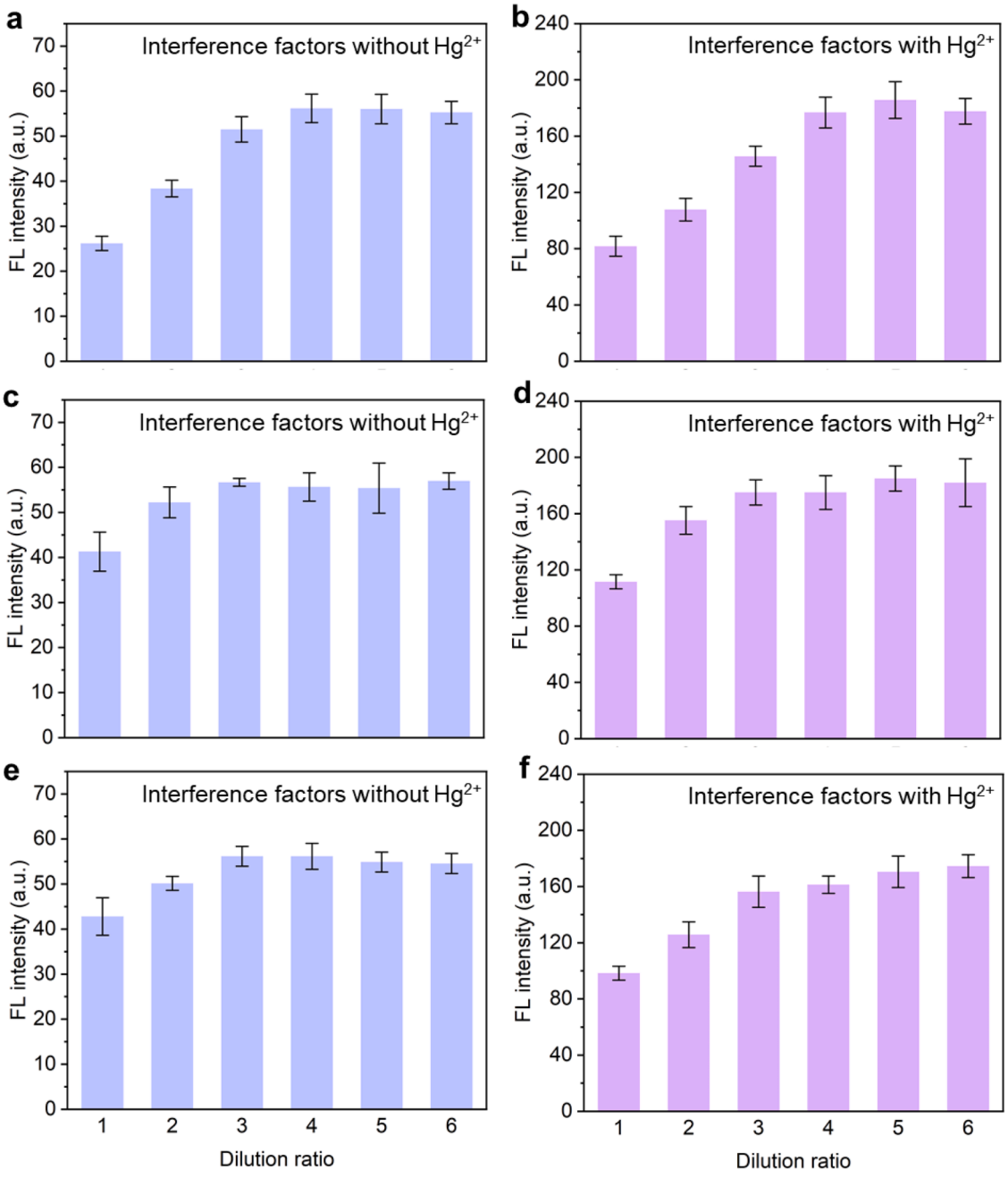

Fig 6. Tolerance level of this method for Hg^{2+} analysis at different dilution ratio of Ca^{2+}, Mg^{2+} and ClO^{-}. (a) Ca^{2+} without Hg^{2+}; (b) Ca^{2+} with Hg^{2+}; (c) Mg^{2+} without Hg^{2+}; (d) Mg^{2+} with Hg^{2+}; (e) ClO^{-} without Hg^{2+}; and (f) ClO^{-} with Hg^{2+}.

MSO-Hg^{2+} system first increased and then decreased. When pH was 7.2, with F/F_0 as the standard, the SNR was at its maximum value. Notably, SGI was reported to be the most sensitive when pH was in the range of 7.5-8.0, however, considering that pH also affected the conformation of MSO, hence its recognition capability towards Hg^{2+} [34], the buffer with pH 7.2 was finally concluded as the best pH value.

Ionic strength is one of the most important factors for a Hg^{2+} biosensor, because it not only determines the hybridization efficiency and stability of DNA double strands, but also affects the formation of T-Hg^{2+}-T structure [35]. Therefore, in our study, the impact of different $NaNO_3$ concentrations on Hg^{2+} detection was also investigated (**Fig 3**d). The reaction conditions were set as follows: $C_{Hg} = 40$ nM, SGI = 1 ×, 100 mM MOPS buffer (with different concentrations of $NaNO_3$), pH = 7.2, T-Hg^{2+}-T reaction time of 5 min, and SGI and MSO-Hg^{2+} incubation time of 2 min. The fluorescence intensity of the two groups with and without the addition of Hg^{2+} both decreased significantly with increasing $NaNO_3$ concentration. Previous work proved that ionic strength had impact on both the fluorescence of SGI and the conformation of MSO sequence; and the optimal ionic strength was various for different nucleic acid affinity materials [34–36]. In terms of the fluorescence intensity ratio F/F_0 with and without the addition of Hg^{2+}, the SNR was the best when the $NaNO_3$ concentration was 250 mM. Thus, the experiment determined that the salt concentration of 250mM was the optimal concentration.

3.3.3. *Optimization of reaction time and incubation time*

The effect of T-Hg^{2+}-T reaction time on Hg^{2+} detection was investigated (**Fig 3**e). C_{Hg} = 40 nM, SGI = 1 ×, 100 mM MOPS buffer (including 250 mM $NaNO_3$), pH = 7.2, and SGI and MSO-Hg^{2+} incubation time of 2 min. Fluorescence intensity of SGI no longer increased

Table 3
Recovery results of Hg^{2+} detection in environmental water samples by using the developed biosensor and ICP-MS

Sample	Added (nM)	ICP-MS		This work	
		Measured (nM)	Recoveries (%)	Measured (nM)	Recoveries (%)
Danjiangkou Reservoir	10	9.78 ±0.26	97.8±2.60	10.18 ±0.54	101.8 ±5.36
	50	51.33 ±0.46	102.7 ±0.92	48.35 ±3.01	96.7±6.02
	100	97.62 ±0.92	97.6±0.92	94.70 ±5.35	94.7±5.35
Hetang Lake	10	9.57 ±0.02	95.7±0.20	9.26 ±0.20	92.6±1.99
	50	50.32 ±0.75	100.6 ±1.50	46.01 ±1.21	92.0±2.42
	100	105.46 ±1.05	105.5 ±1.05	90.81 ±14.10	90.8±14.1
Groundwater at Tsinghua Campus	10	10.21 ±0.12	102.1 ±1.20	8.93 ±0.52	89.3±5.16
	50	48.20 ±0.48	96.4±0.96	45.85 ±3.82	91.7±7.65
	100	104.33 ±0.74	104.3 ±0.74	82.83 ±5.71	82.8±5.71

after reacting for 5min, indicating that the T-Hg^{2+}-T base pair had been formed and SGI had been fully embedded in the hairpin type structure. Hence, 5min was chosen as the best reaction time.

The incubation time of SGI and MSO has a significant influence on detection performance. Under the optimized reaction conditions, the incubation time was investigated (Fig 3f). The reaction conditions were set as follows: $C_{Hg} = 40$ nM, SGI = 1 ×, 100 mM MOPS buffer (including 250 mM $NaNO_3$), pH = 7.2, and T-Hg^{2+}-T reaction time of 5 min. When the reaction time reached 2 min, the fluorescence intensity stopped increasing and was observed to be relatively stable. When the reaction time exceeded 6 min, the fluorescence intensity began to diminish. Therefore, 2 min was finally elected as the best reaction time for SGI and MSO.

3.4. Detection of Hg^{2+} using MSO and SGI

The method for the determination of Hg^{2+} was established based on the above principles and optimizations. Under optimized experimental conditions, the addition of Hg^{2+} gradually enhanced the fluorescence intensity of SGI, which was linearly correlated with the concentration of Hg^{2+} (Fig 4). The linear standard curve was $FL = 1.307C_{Hg} + 47.17$, $R^2 = 0.994$, and the linear range was 10-100 nM. A specific Hg^{2+} concentration, which yielded the signal equal to three times of the standard deviation (3σ) of the biosensor response to the blank sample without Hg^{2+} addition, was defined as the limit of detection (LOD). Following the 3σ rule, LOD of this technology was calculated to be 0.68 nM, and the relative standard deviation was 2.33% for 11 parallel measurements of 10 nM Hg^{2+}. The performance of the developed Hg^{2+} biosensor with other reported fluorescent Hg^{2+} sensors was listed in Table 2 for comparison. Compared to the previous studies, our technology achieved the comparable LOD and quantification range. Notably, when facing the high Hg^{2+}-contaminated samples, it is suggested to dilute the samples using ultrapure water.

3.5. Selectivity of Hg^{2+} detection

Fig 5 corresponds to the response of metal ions and anions in Table 1 and the typical fluorescent spectra under different conditions were demonstrated in **Fig S1**, accordingly. As shown in Fig 5a, the FL intensity caused by other metal ions was lower than 10% of that responding to 100 nM Hg^{2+} except for Cu^{2+}, which may be caused by the combination of Cu^{2+} and adenine (A) in MSO to interfere with the signal. In the coexistence interference test (Fig 5b), 100 nM Hg^{2+} was mixed with cations and it was found that Al^{3+}, Ag^{+} and MIX had greater interference, which proved that the interference of different metal ions could produce mechanism of synergistic enhancement. The interference of anions was further explored (Fig 5c,d). The response test and coexistence interference test showed that, compared with the fluorescence intensity corresponding to 100 nM Hg^{2+}, NO_3^-, SO_4^{2-}, Cl^- and F^- posed negligible interference on Hg^{2+} detection. Compared with the anions, the cations, including Ni^{2+}, Al^{3+}, Ag^{+} and MIX, showed more negative impacts on the sensing process, causing more than 30% lower than the original signal when coexisting with Hg^{2+} (Fig 5**b**). In other cases, the signal deviation caused by the interferences was less than 15%. As stated, the interfering ions with the concentrations under the majority of the most unfavorable conditions in environmental water were used for investigation. Therefore, it was concluded that the technology was applicable in the majority of the application scenarios of environmental monitoring, however, was not suggested to be used when the concentrations of Ni^{2+}, Al^{3+}, Ag^{+} and their mixture were as high as in Table 1.

The interference of hardness (Ca^{2+} and Mg^{2+}) and ClO^- in water was also studied. The typical fluorescent spectra under different conditions were demonstrated in **Fig S2**, accordingly. Based on the concentrations in Table 1, these three ions were diluted to 1, 2, 3, 4, 5, and 6 multiples to investigate the response to the biosensor and the coexistence interference with Hg^{2+}. As shown in Fig 6a,b, when Ca^{2+} was diluted 4 times or more, its interference with Hg^{2+} became negligible, thus the tolerance of Ca^{2+} was 100 mg/L. Similarly, the tolerance of Mg^{2+} was obtained to be 80 mg/L, i.e., its three-fold dilution (Fig 6c,d), while the tolerance of ClO^- was obtained to be 1 mg/L, i.e., its four-fold dilution (Fig 6e,f). That was to say, the sample was suggested to be diluted three or four folds by using ultra-pure water to achieve the tolerant concentrations before detection if the environmental matrices were under the most unfavorable conditions of Ca^{2+}, Mg^{2+} ClO^-.

3.6. Recovery of Hg^{2+} detection

Similarly, in order to investigate the practical application performance of the developed technology, the contents of Hg^{2+} in two types of environmental surface water (Danjiangkou Reservoir and Hetang Lake in Tsinghua University) and one kind of groundwater (groundwater in Tsinghua University) were investigated, and the standard recovery experiment was carried out. The spiked concentrations of Hg^{2+} were 10, 50 and 100 nM. The spiked recoveries of Hg^{2+} were in the range of 82.8% to 101.8% (Table 3), proving the reliability of the method. Notably, the recovery percentages in the groundwater at Tsinghua Campus were lower than the values in other two kinds of surface water. We attributed this phenomenon to the high hardness, i.e. in the range of 290–350 mg/L in calcium carbonate, in groundwater matrix compared with the surface water matrix although the pretreatment was adopted to eliminate the effect of hardness, including boiling the water samples to precipitate the carbonate hardness, cooling the samples to room temperature and filtering them through a filter with a 0.22 μm nylon membrane, and then diluting twice using ultra-pure water before the recovery experiments [29]. Besides, compared with the ICP-MS results with the spiked recoveries in the range of 95.7% to 105.5%, the biosensor technology showed less stability in applications, however was more feasible, low-cost and simple-to-use, hence with great potentials for in field detection than other instrumental analysis technologies.

4. Conclusions

In summary, we have successfully designed a selective and sensitive method for detection of Hg^{2+} by using SGI and MSO. In the presence of Hg^{2+}, the randomly coiled MSO folds into a hairpin-like structure by T-Hg^{2+}-T mismatch, which interacts strongly with SGI, thereby generating a fluorescence turn-on signal. Under optimized conditions, the linear range of Hg^{2+} detection is 10–100 nM and the LOD is 0.68 nM. Additionally, the sensing system features both high sensitivity and

selectivity. The recoveries of Hg^{2+} in environmental samples were in the range of 82.8% to 101.8%, making it possible for in-field and real-time detection. Owing to its low cost and convenient operation, our method establishes the groundwork for the development of a highly competitive portable water-pollution detector.

Declaration of Competing Interest

The authors declare that they have no known competing financial interests or personal relationships that could have appeared to influence the work reported in this paper.

Acknowledgment

This research was funded by the National Key Research and Development Program of China (2019YFD1100505), and the Tsinghua-Hach joint project (20133000129).

Supplementary materials

Supplementary material associated with this article can be found, in the online version, at doi:10.1016/j.snr.2022.100101.

References

[1] T. Kokab, A. Shah, F.J. Iftikhar, J. Nisar, M.S. Akhter, S.B. Khan, Amino acid-fabricated glassy carbon electrode for efficient simultaneous sensing of zinc(II), cadmium(II), copper(II), and mercury(II) ions, ACS Omega 4 (2019) 22057–22068.
[2] Y. Zhang, T. Yan, L. Yan, X. Guo, L. Cui, Q. Wei, B. Du, Preparation of novel cobalt ferrite/chitosan grafted with graphene composite as effective adsorbents for mercury ions, J. Mol. Liq. 198 (2014) 381–387.
[3] G. Maduraiveeran, M. Sasidharan, V. Ganesan, Electrochemical sensor and biosensor platforms based on advanced nanomaterials for biological and biomedical applications, Biosens. Bioelectron. 103 (2018) 113–129.
[4] H.N. Kim, W.X. Ren, J.S. Kim, J. Yoon, Fluorescent and colorimetric sensors for detection of lead, cadmium, and mercury ions, Soc. Rev. 41 (2011) 3210–3244.
[5] C.J. Horng, Simultaneous determination of urinary zinc, cadmium, lead and copper concentrations in steel production workers by differential-pulse anodic stripping voltammetry, Analyst 121 (1996) 1511–1514.
[6] V.Y. Maldonado, P.J. Espinoza-Montero, C.A. Rusinek, G.M. Swain, Analysis of Ag (I) biocide in water samples using anodic stripping voltammetry with a boron-doped diamond disk electrode, Anal. Chem. 90 (2018) 6477–6485.
[7] A.G. Memon, Y. Xing, X. Zhou, R. Wang, L. Liu, S. Zeng, M. He, M. Ma, Ultrasensitive colorimetric aptasensor for Hg2+ detection using Exo-III assisted target recycling amplification and unmodified AuNPs as indicators, J. Hazard. Mater. 384 (2020), 120948.
[8] R. Wang, X. Zhou, H. Shi, Y. Luo, T-T mismatch-driven biosensor using triple functional DNA-protein conjugates for facile detection of Hg2+, Biosens. Bioelectron. 78 (2016) 418–422.
[9] Q. Zhu, L. Liu, Y. Xing, X. Zhou, Duplex functional G-quadruplex/NMM fluorescent probe for label-free detection of lead(II) and mercury(II) ions, J. Hazard. Mater. 355 (2018) 50.
[10] C. Wang, Y. Li, Y. Zhu, X. Zhou, Q. Lin, M. He, High-k solid-gate transistor configured graphene biosensor with fully integrated structure and enhanced sensitivity, Adv. Funct. Mater. 26 (2016) 7668.
[11] Y. Zhou, H. Wang, D. Song, Z. Li, S. Han, F. Long, A. Zhu, Simple, rapid, and sensitive on-site detection of Hg2+ in water samples through combining portable evanescent wave optofluidic biosensor and fluorescence resonance energy transfer principle, Anal. Chim. Acta 1155 (2021), 338351.
[12] M. Ebrahimi, J.B. Raoof, R. Ojani, Sensitive electrochemical DNA-based biosensors for the determination of Ag^{+} and Hg^{2+} ions and their application in analysis of amalgam filling, J. Iran. Chem. Soc. 15 (2018) 1871–1880.
[13] X. Li, Z. Du, S. Lin, J. Tian, H. Tian, W. Xu, ExoIII and TdT dependent isothermal amplification (ETDA) colorimetric biosensor for ultra-sensitive detection of Hg2+, Food Chem 316 (2020), 126303.
[14] H Khani, S Abbasi, M Tavakkoli Yaraki, Y.N Tan, A naked-eye colorimetric assay for detection of Hg^{2+} ions in real water samples based on gold nanoparticles-catalyzed clock reaction, J. Mol. Liq. 345 (2022), 118243.
[15] A.D. Ellington, J.W. Szostak, In vitro selection of RNA molecules that bind specific ligands, Nature 346 (1990) 818–822.
[16] J. Liu, Z. Cao, Y. Lu, Functional nucleic acid sensors, Chem. Rev. 109 (2009) 1948–1998.
[17] A. Ono, H. Togashi, Highly selective oligonucleotide-based sensor for mercury(II) in aqueous solutions, Angew. Chem. Int. Edit. 43 (2004) 4300–4302.
[18] T. Li, E. Wang, S. Dong, Potassium−lead-switched g-quadruplexes: a new class of DNA logic gates, J. Am. Chem. Soc. 131 (2009) 15082–15083.
[19] F. Long, C. Gao, H.C. Shi, M. He, A.N. Zhu, A.M. Klibanov, A.Z. Gu, Reusable evanescent wave DNA biosensor for rapid, highly sensitive, and selective detection of mercury ions, Biosens. Bioelectron. 26 (2011) 4018–4023.
[20] J. Li, Y. Lu, A highly sensitive and selective catalytic DNA biosensor for lead ions, J. Am. Chem. Soc. 122 (2000) 10466–10467.
[21] A.G. Memon, X. Zhou, J. Liu, R. Wang, L. Liu, B. Yu, M. He, H. Shi, Utilization of unmodified gold nanoparticles for label-free detection of mercury (II): insight into rational design of mercury-specific oligonucleotides, J. Hazard. Mater. 321 (2017) 417–423.
[22] R. Wang, X. Zhou, H. Shi, Triple functional DNA–protein conjugates: signal probes for Pb2+ using evanescent wave-induced emission, Biosens. Bioelectron. 74 (2015) 78–84.
[23] J.R. Zhang, W.T. Huang, A.L. Zeng, H.Q. Luo, N.B. Li, Ethynyl and π-stacked thymine–Hg2+–thymine base pairs enhanced fluorescence quenching via photoinduced electron transfer and simple and sensitive mercury ion sensing, Biosens. Bioelectron. 64 (2015) 597–604.
[24] H. Qiu, N. Wu, Y. Zheng, M. Chen, S. Weng, Y. Chen, X. Lin, A robust and versatile signal-on fluorescence sensing strategy based on SYBR Green I dye and graphene oxide, Int. J. Nanomed. 10 (2015) 147–156.
[25] S. Han, X. Zhou, Y. Tang, M. He, X. Zhang, H. Shi, Y. Xiang, Practical, highly sensitive, and regenerable evanescent-wave biosensor for detection of Hg2+ and Pb2+ in water, Biosens. Bioelectron. 80 (2016) 265–272.
[26] M. Zhang, H. Le, X. Jiang, B. Ye, Molecular beacon"-directed fluorescence of Hoechst dyes for visual detection of Hg(II) and biothiols and its application for a logic gate, Chem. Commun. 49 (2013) 2133–2135.
[27] D. Li, S. Song, C. Fan, Target-responsive structural switching for nucleic acid-based sensors, Accounts Chem. Res. 43 (2010) 631–641.
[28] Y. Li, N. Liu, H. Liu, Y. Wang, Y. Hao, X. Ma, X. Li, Y. Huo, J. Lu, S. Tang, C. Wang, Y. Zhang, Z. Gao, A novel label-free fluorescence assay for one-step sensitive detection of Hg2+ in environmental drinking water samples, Sci. Rep. 7 (2017) 45974.
[29] X. Zhou, A.G. Memon, W. Sun, F. Fang, J. Guo, Fluorescent probe for Ag+ detection using sybr green I and C-C mismatch, Biosensors 11 (2021) 6.
[30] J. Wang, B. Liu, Highly sensitive and selective detection of Hg2+ in aqueous solution with mercury-specific DNA and sybr green I, Chem. Commun. (2008) 4759–4761.
[31] D. Tan, Y. He, X. Xing, Y. Zhao, H. Tang, D. Pang, Aptamer functionalized gold nanoparticles based fluorescent probe for the detection of mercury (II) ion in aqueous solution, Talanta 113 (2013) 26–30.
[32] L. Zhang, T. Li, B. Li, J. Li, E. Wang, Carbon nanotube–DNA hybrid fluorescent sensor for sensitive and selective detection of mercury(II) ion, Chem. Commun. 46 (2010) 1476–1478.
[33] F. Yang, M. Zhao, B. Zheng, D. Xiao, L. Wu, Y. Guo, Influence of pH on the fluorescence properties of graphene quantum dots using ozonation pre-oxide hydrothermal synthesis, J. Mater. Chem. 22 (2012) 25471–25479.
[34] T. Hianik, V. Ostatná, M. Sonlajtnerova, I. Grman, Influence of ionic strength, pH and aptamer configuration for binding affinity to thrombin, Bioelectrochemistry 70 (2007) 127–133.
[35] S. Yu, W. Li, Y. Fujii, T. Omura, H. Minami, Fluorescent spherical sponge cellulose sensors for highly selective and semiquantitative visual analysis: detection of Hg^{2+} and Cu^{2+} ions, ACS Sustain. Chem. Eng. 7 (2019) 19157–19166.
[36] J. Liu, Y. Lu, Non-base pairing DNA provides a new dimension for controlling aptamer-linked nanoparticles and sensors, J. Am. Chem. Soc. 129 (2007) 8634–8643.
[37] S. Kokilavani, A. Syed, A.M. Thomas, N. Marraiki, S. Al-Rashed, A.M. Elgorban, L. L. Raju, A. Das, S.S. Khan, Polyethylene glycol functionalised Ag NPs based optical probe for the selective and sensitive detection of Hg(II), J. Mol. Liq. 307 (2020), 112978.
[38] S. Balasurya, A. Syed, M. Swedha, G. Harini, A.M. Elgorban, N.S.S. Zaghloul, A. Das, S.S. Khan, A novel SPR based Fe@Ag core-shell nanosphere entrapped on starch matrix an optical probe for sensing of mercury(II) ion: a nanomolar detection, wide pH range and real water sample application, Spectrochim. Acta A 263 (2021), 120204.
[39] H.-B. Wang, H.-Y. Bai, Y.-S. Wang, T. Gan, Y.-M. Liu, Highly selective fluorimetric and colorimetric sensing of mercury(II) by exploiting the self-assembly-induced emission of 4-chlorothiophenol capped copper nanoclusters, Microchim. Acta 187 (2020) 185.
[40] H.-B. Wang, Y. Chen, Y. Li, H.-D. Zhang, J.-T. Cao, A rapid, sensitive and label-free sensor for Hg(ii) ion detection based on blocking of cysteine-quenching of fluorescent poly(thymine)-templated copper nanoparticles, RSC Adv 5 (2015) 94099–94104.
[41] K. Karthikeyan, L. Sujatha, Fluorometric sensor for mercury ion detection in a fluidic MEMS device, IEEE Sens. J. 18 (2018) 5225–5231.